Molecular Therapy
Original Article

DUX4 Transcript Knockdown with Antisense 2′-*O*-Methoxyethyl Gapmers for the Treatment of Facioscapulohumeral Muscular Dystrophy

Kenji Rowel Q. Lim,[1] Adam Bittel,[2] Rika Maruyama,[1] Yusuke Echigoya,[3] Quynh Nguyen,[1] Yiqing Huang,[1] Kasia Dzierlega,[1] Aiping Zhang,[2] Yi-Wen Chen,[2,4] and Toshifumi Yokota[1,5]

[1]Department of Medical Genetics, Faculty of Medicine and Dentistry, University of Alberta, Edmonton, AB T6G2H7, Canada; [2]Center for Genetic Medicine Research, Children's National Health System, Washington, DC 20010, USA; [3]Laboratory of Biomedical Science, Department of Veterinary Medicine, College of Bioresource Sciences, Nihon University, Fujisawa, Kanagawa 252-0880, Japan; [4]Department of Genomics and Precision Medicine, School of Medicine and Health Science, George Washington University, Washington, DC 20052, USA; [5]Muscular Dystrophy Canada Research Chair, Edmonton, AB T6G2H7, Canada

Facioscapulohumeral muscular dystrophy (FSHD) is an autosomal dominant disorder characterized by a progressive, asymmetric weakening of muscles, starting with those in the upper body. It is caused by aberrant expression of the *double homeobox protein 4* gene (*DUX4*) in skeletal muscle. FSHD is currently incurable. We propose to develop a therapy for FSHD using antisense 2′-*O*-methoxyethyl (2′-MOE) gapmers, to knock down *DUX4* mRNA expression. Using immortalized patient-derived muscle cells and local intramuscular injections in the *FLExDUX4* FSHD mouse model, we showed that our designed 2′-MOE gapmers significantly reduced *DUX4* transcript levels *in vitro* and *in vivo*, respectively. Furthermore, *in vitro*, we observed significantly reduced expression of DUX4-activated downstream targets, restoration of FSHD signature genes by RNA sequencing, significant improvements in myotube morphology, and minimal off-target activity. This work facilitates the development of a promising candidate therapy for FSHD and lays down the foundation for *in vivo* systemic treatment studies.

INTRODUCTION

Facioscapulohumeral muscular dystrophy (FSHD) is the third most common form of muscular dystrophy in the world, with 1:8,000–22,000 people affected globally.[1,2] FSHD is a disabling, autosomal dominant disorder primarily characterized by progressive muscle weakness that begins in the face, shoulders, and upper limbs, followed by the lower extremities.[1] Muscle involvement in FSHD is distinctly asymmetric, with disease severity varying across individuals. Around 15%–20% of patients are wheelchair-bound.[3] In certain cases, often in early-onset FSHD, patients present with additional extra-muscular features, e.g., hearing loss, retinal vasculopathy, and cognitive impairment.[4–6] Surgery and physical therapy, among others, are available to help manage symptoms and improve patient quality of life.[7] However, these approaches do not treat FSHD itself, and the disease remains incurable at present.

FSHD is caused by mutations promoting aberrant expression of the *double homeobox protein 4* gene (*DUX4*) in skeletal muscle. On chromosome 4q35, there is a macrosatellite array of 3.3-kb D4Z4 repeats that is typically 11–100 repeats long in healthy individuals. Each D4Z4 unit contains the first two exons of the *DUX4* gene.[8] Its third and final exon is found immediately after the most distal unit of the array and possesses a functional polyadenylation signal (PAS) only in the 4qA haplotype.[9] The presence of the PAS is required for successful *DUX4* transcription. In most tissues, including skeletal muscle, the D4Z4 array is normally hypermethylated after early embryonic development, silencing *DUX4* expression.[10,11] However, in FSHD, D4Z4 methylation is reduced either through contraction of the array, mutations in genes coding for epigenetic regulators, or a combination of both.[1,9,11–13] It is now known that strict cutoffs of 4q35 D4Z4 array length (i.e., $\leq$10 repeats) do not satisfactorily explain penetrance of the FSHD phenotype. For instance, individuals with less than 10 repeat units in this array can be asymptomatic.[12] Although further study of the underlying genetics in this disease is warranted, it remains that these culminate in the de-repression of *DUX4*, which produces the DUX4 transcription factor whose downstream activities are thought to cause FSHD.[14]

Given its central role in FSHD, reducing *DUX4* expression has been the focus of a number of therapies being developed for the disease. This was mostly achieved through the use of antisense oligonucleotides (AOs), such as those of the phosphorodiamidate morpholino oligomer (PMO) and 2′-*O*-methyl RNA (2′-OMe) chemistries. PMOs and 2′-OMe AOs were previously designed to target the *DUX4* PAS[15,16] or its splice sites,[17,18] respectively. Both resulted in up to 50% reduced *DUX4* transcript levels *in vitro*, as well as considerable decreases in *DUX4* expression *in vivo* in xenograft and

Received 1 June 2020; accepted 12 October 2020;
https://doi.org/10.1016/j.ymthe.2020.10.010.

Correspondence: Toshifumi Yokota, Department of Medical Genetics, Faculty of Medicine and Dentistry, University of Alberta, Edmonton, AB T6G2H7, Canada.
E-mail: toshifumi.yokota@ualberta.ca
Correspondence: Yi-Wen Chen, Center for Genetic Medicine Research, Children's National Health System, Washington, DC 20010, USA.
E-mail: ychen@childrensnational.org

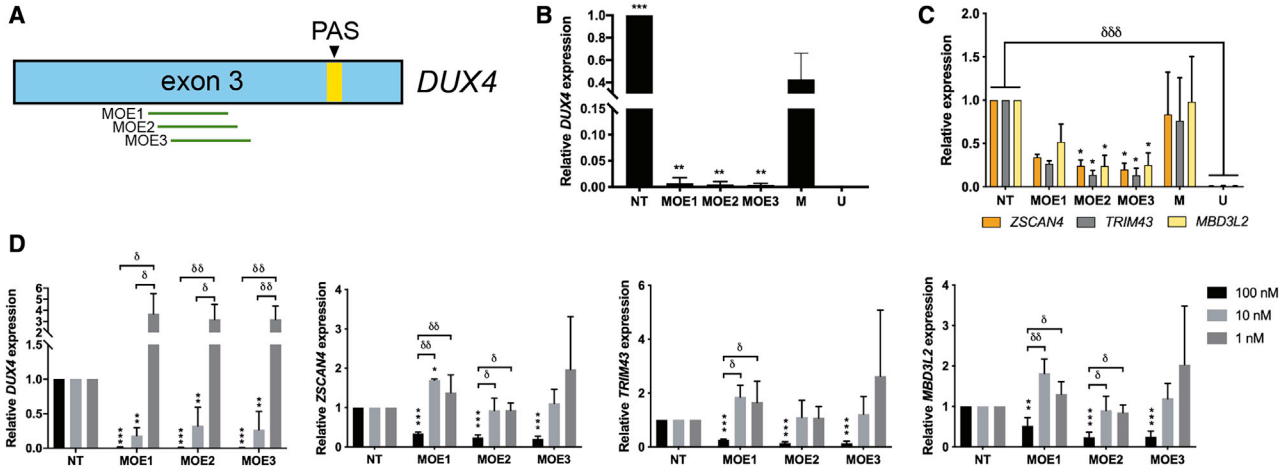

Figure 1. *DUX4* Knockdown Efficacy Evaluation of Designed 2′-MOE Gapmers

(A) Scheme showing the approximate locations targeted by our 2′-MOE gapmers on *DUX4* exon 3. Transcript levels of (B) *DUX4* and (C) *ZSCAN4*, *TRIM43*, and *MBD3L2* were evaluated by quantitative real-time RT-PCR after overnight treatment of immortalized FSHD patient-derived myotubes with 100 nM of the 2′-MOE gapmers at 13 days post-differentiation. *p < 0.05, **p < 0.005, ***p < 0.0005 versus mock (M), one-way ANOVA with Dunnett's test. $^{\delta\delta\delta}$p < 0.0005, unpaired, two-tailed t test. (D) Transcript levels of these same four genes after treatment with 100, 10, or 1 nM of the 2′-MOE gapmers, following similar culture conditions. Error bars: SD; n = 3 independent experiments. **p < 0.005, ***p < 0.0005 versus NT, one-way ANOVA with Dunnett's test. $^{\delta}$p < 0.05, $^{\delta\delta}$p < 0.005, one-way ANOVA with Tukey's test. NT, non-treated; PAS, polyadenylation signal; U, FSHD-unaffected/healthy.

DUX4-transduced mouse models. More effective *DUX4* knockdown is desirable, however, because it is known that low levels of *DUX4* expression are sufficient to drive pathological changes in skeletal muscle.[19] Compared with PMOs and 2′-OMe AOs, which passively knock down gene expression by interfering with *DUX4* transcript maturation, use of antisense gapmers may prove more effective owing to their ability to actively induce the degradation of target mRNA transcripts via RNase H.

In the present study, we therefore aimed to explore the efficacy of antisense gapmers for *DUX4* knockdown, specifically those with the 2′-*O*-methoxyethyl (2′-MOE) modification. The 2′-MOE chemistry has proved to be favorable for therapeutic AO development, with its enhanced resistance to nucleases, increased target binding affinity and specificity, as well as with four 2′-MOE-based AOs already having received approval in the United States and/or the European Union.[20–23] We designed 2′-MOE gapmers against mRNA in the coding region of *DUX4* and evaluated their efficacy and specificity using immortalized FSHD patient-derived muscle cells as an *in vitro* model. We then test these gapmers *in vivo* via local intramuscular (i.m.) treatment in *FLExDUX4* FSHD model mice.[24] Overall, we show that our 2′-MOE gapmers are potent agents of *DUX4* transcript knockdown and serve as promising clinical trial candidates for FSHD therapy.

RESULTS

Designed 2′-MOE Gapmers Effectively Knock Down DUX4 Transcript Expression

Three 2′-MOE gapmers were designed and tested for their potential to knock down *DUX4* transcript levels (Figure 1A; Table 1). The 2′-MOE gapmers were transfected at 100 nM into immortalized FSHD patient-derived muscle cells at 13 days post-differentiation, and cells were collected the following day for analysis. Quantitative real-time RT-PCR expression analysis revealed that all three 2′-MOE gapmers significantly reduced *DUX4* transcript levels almost completely (n = 3; p < 0.005) (Figure 1B). No significant differences in knockdown efficacy were observed between the gapmers. Significant knockdown of the expression of DUX4 downstream transcriptional targets *ZSCAN4*, *TRIM43*, and *MBD3L2* was observed for MOE2 and MOE3 (n = 3; p < 0.05) (Figure 1C). Transfection of lower doses of the 2′-MOE gapmers led to significant *DUX4* transcript knockdown at the 10 nM, but not the 1 nM, dose (n = 3; p < 0.005) (Figure 1D). Up to ∼70% reduction in *DUX4* levels on average was observed upon treatment with 10 nM of the 2′-MOE gapmers. *ZSCAN4*, *TRIM43*, and *MBD3L2* expression levels were not affected at the 10 and 1 nM transfected doses of any of the 2′-MOE gapmers, however. Interestingly, treatment with lower doses of some of the 2′-MOE gapmers led to variably increased expression of *DUX4* and its downstream target genes compared with the non-treated control, particularly at the 1 nM transfected concentration (Figure 1D). Overall, these results show that the designed 2′-MOE gapmers could knock down *DUX4* transcript levels with high efficacy *in vitro*, even at reduced doses.

A Subset of Transcriptome-Level Alterations Was Restored with 2′-MOE Gapmer Treatment

To obtain a better idea of the restorative effects of 2′-MOE gapmer treatment at the transcriptomic level, we performed RNA sequencing analysis on total RNA extracts from immortalized healthy control myotubes and patient-derived myotubes that were either treated or

Table 1. Characteristics of Designed 2′-MOE Gapmers against the *DUX4* Transcript

ID	Sequence[a] (5′–3′)	Length (nt)	Target *DUX4* Exon	GC Content (%)
MOE1	**TAGAC**AGCGTCGGAA**GGTGG**	20	3	60.0
MOE2	**CTAGA**CAGCGTCGGA**AGGTG**	20	3	60.0
MOE3	**CCTAG**ACAGCGTCGG**AAGGT**	20	3	60.0

[a]Fully phosphorothioated. Bold indicates 2′-MOE nucleotides, and nonbold indicates DNA.

not with MOE3. MOE3 was chosen because it induced the greatest reduction in *DUX4* transcript expression in our initial screen (Figure 1B). For the treatment, cells were transfected with 100 nM MOE3 at 13 days post-differentiation and harvested the following day, similar to what we did in the initial 2′-MOE gapmer screen. To obtain a list of transcripts linked to *DUX4* expression, we compared our dataset with that of Rickard et al.,[25] who performed RNA sequencing on extracts from flow cytometry-sorted DUX4 reporter-positive primary FSHD patient myotubes and who used similar cell culture conditions as we did in this study. We initially obtained 96 overlapping transcripts with that of the Rickard et al.[25] dataset but excluded 2 because parameters for these were not present in all pairwise comparisons across our groups (Figure 2A). This led us to an FSHD signature of 94 transcripts whose expression levels were significantly affected by *DUX4* expression ($n = 3$; $p < 0.05$) that consisted of 69 upregulated and 25 downregulated transcripts, representing 55 and 18 genes, respectively. A comparison of the expression levels obtained for these transcripts between our study and that of Rickard et al.[25] revealed that the majority of genes had a similar direction of dysregulation (up/down) in both datasets (Figure 2B). We found that MOE3 treatment restored the expression of some FSHD signature transcripts to healthy levels (Figures 2C and 2D). Specifically, MOE3 significantly restored the expression of 8/69 (12%) upregulated FSHD transcripts and 1/25 (4%) downregulated transcripts ($n = 3$; $p < 0.05$), all corresponding to unique genes (Table S1). Of the significantly restored upregulated transcripts, two were validated by quantitative real-time RT-PCR (*ZSCAN4* and *TRIM43*; Figure 1C); an additional four upregulated transcripts (*MBD3L2*, *TRIM48*, *TRIM64B*, *PRAMEF4/5/9/11*) that showed non-significant restoration in RNA sequencing were demonstrated to have significantly reduced expression post-treatment by quantitative real-time RT-PCR (Figure 1C; Figure S1; Table S2).

Improvements in Cellular Phenotypes upon 2′-MOE Gapmer Treatment

Myotube fusion and size are two phenotypes negatively affected by aberrant *DUX4* expression and signaling in skeletal muscle.[14,26,27] We sought to determine whether 2′-MOE gapmer treatment could promote increased muscle fusion and decreased hypotrophic characteristics *in vitro*. Qualitatively, immunocytochemistry showed that immortalized FSHD patient-derived muscle cells treated with 10 nM of the 2′-MOE gapmers had larger, extensive myotubes with more nuclei than the non-treated or mock gapmer-treated controls (Figure 3A). All 2′-MOE gapmer-treated muscle cells had significantly increased myogenic fusion indices (MFIs), reaching up to 55% higher MFIs on average than the mock control ($n = 3$; $p < 0.05$) (Figure 3B). No significant MFI differences were observed across the gapmer-treated groups. Myotube diameters were also significantly increased by the treatment ($n = 3$; $p < 0.0005$), shifting the frequency distribution peak from 15–20 to 20–25 μm, similar to that of the healthy control (Figures 3C and 3D). Once again, no significant differences in myotube diameters were observed between gapmer-treated groups. Moreover, western blot analysis revealed that myosin heavy chain protein levels were observably but non-significantly increased by treatment with 100 nM MOE3 compared with mock-treated controls ($n = 3$; $p = 0.0828$) (Figure S2). We saw no effect of 10 nM 2′-MOE gapmer treatment on muscle cell apoptosis, another *in vitro* phenotype that characterizes FSHD (Figure 3E).[14,28]

Off-Target Effect Analysis of 2′-MOE Gapmer Treatment

Using GGGenome, we compiled a list of sequences from other genes sharing the highest degree of similarity possible to the *DUX4* target sequence of our 2′-MOE gapmers (Table 2). In part due to the length of the 2′-MOE gapmers, the closest sequences we could find were those having at least a 3-bp mismatch to the targeted *DUX4* sequence. We examined whether the expression levels of these genes were knocked down upon 100 nM 2′-MOE gapmer treatment in immortalized FSHD patient-derived cells. Upon further testing, only *BANF1*, *SSR4*, *FARP1*, and *ZBTB7B* had detectable expression in FSHD patient-derived myotubes. Treatment with the 2′-MOE gapmers did not significantly reduce the transcript levels of these genes, except for *BANF1*, which was significantly knocked down by MOE1 and MOE2 ($n = 3$; $p < 0.05$ and $p < 0.005$, respectively) (Figures 4A–4D). MOE1 treatment also significantly increased the expression of *ZBTB7B* ($n = 3$; $p < 0.005$). However, by the nature of the change, this is not considered a direct off-target effect resulting from gapmer-mediated knockdown. Importantly, we note that the expression levels of all four potential off-target genes were not affected by MOE3.

2′-MOE Gapmer Treatment Reduces DUX4 Expression in an FSHD Mouse Model

FLExDUX4 mice carry a floxed human full-length *DUX4* transgene and express very low levels of *DUX4* transcript even without Cre-mediated induction.[24] To determine the *in vivo* efficacy of local 2′-MOE gapmer treatment, we treated adult hemizygous *FLExDUX4* mice with 20 μg i.m. injections of MOE3 to the tibialis anterior (TA) every other day

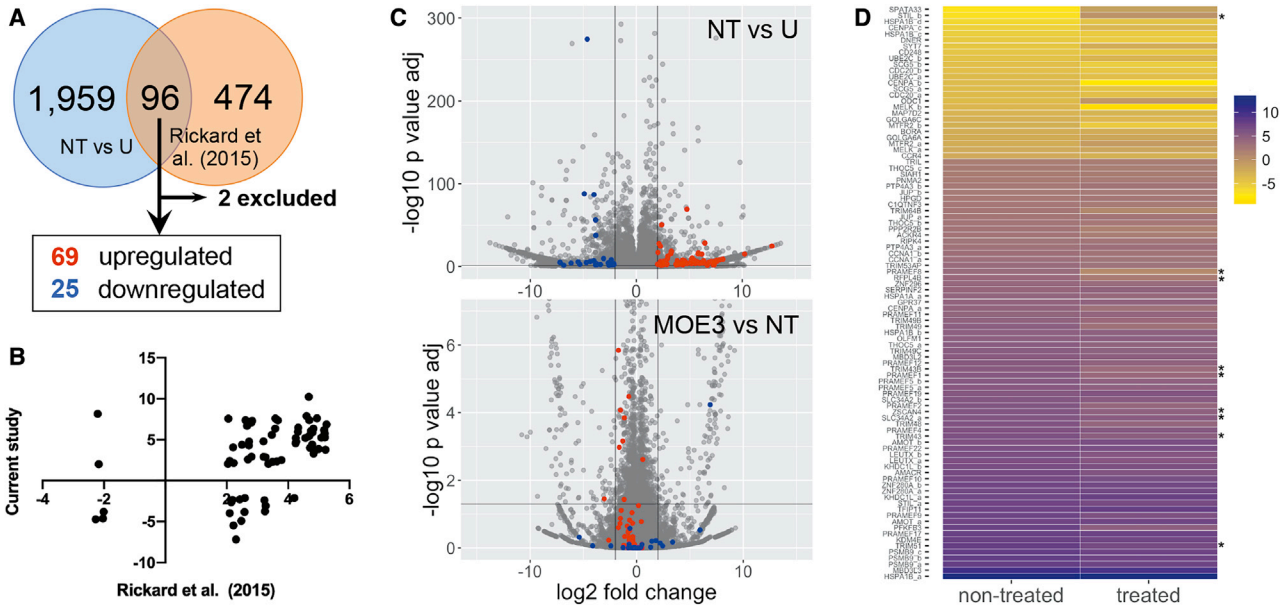

Figure 2. RNA Sequencing Analysis of 2′-MOE Gapmer-Treated Muscle Cells

(A) FSHD signature transcripts from comparison with the RNA sequencing results of Rickard et al.,[25] who used DUX4 reporter-positive primary FSHD patient myotubes. (B) Plot of $\log_2$(fold change) values (cutoff ± 2) for unique genes in the current study versus values obtained by Rickard et al.[25] For genes with multiple transcripts in our dataset, the transcript with the least adjusted p value was used to represent the gene. (C) Volcano plot visualizations of RNA sequencing results from our dataset. Comparisons are indicated in the upper right, with the second listed sample as the reference. FSHD signature transcripts are shown as colored dots: upregulated (red) and downregulated (blue). The horizontal line represents the cutoff adjusted p value of 0.05, and the vertical lines represent $\log_2$(fold change) values of ±2. (D) Heatmap visualization of the expression levels of the 94 FSHD signature transcripts before and after treatment with 100 nM MOE3. Expression levels are colored from high to low with purple to yellow shades, respectively. Asterisks indicate transcripts significantly restored ($p < 0.05$) to healthy levels. n = 3 independent experiments. See also Figure S1.

for 6 days. MOE3 was chosen given its increased capacity to reduce *DUX4* transcript expression as previously mentioned and also from its favorable performance in the off-target effect analysis. For each mouse, MOE3 was injected in one of the legs, while vehicle (phosphate-buffered saline [PBS]) was injected in the other. Quantitative real-time RT-PCR was performed to determine *DUX4* expression levels a day after the third injection; because the low level of *DUX4* expression in *FLExDUX4* mice is not sufficient to induce DUX4 downstream genes,[24] we were not able to evaluate for their expression in this experiment. Our results showed that injection of MOE3 into the TA of *FLExDUX4* mice significantly reduced *DUX4* mRNA expression compared with the contralateral limb that received only a PBS injection (n = 5; $p < 0.05$) (Figure 5). Similar injection of a scrambled 2′-MOE gapmer control did not have an effect on *DUX4* mRNA expression in *FLExDUX4* mice; MOE3 significantly knocked down *DUX4* transcript levels compared with the scrambled control (n = 5 MOE3-treated mice, n = 3 scrambled gapmer-treated mice; $p < 0.05$).

DISCUSSION

Since initial demonstrations of their effective knockdown abilities *in vitro*,[29,30] 2′-MOE gapmers have proceeded to become one of the most successful AO chemistries in clinical development. Two AO gapmers have been given US Food and Drug Administration (FDA) approval thus far: mipomersen (Kynamro; Ionis) for familial hypercholesterolemia and inotersen (Tegsedi; Akcea) for hereditary transthyretin amyloidosis, both of which are of the 2′-MOE chemistry.[21,31,32] A third, volanesorsen (Waylivra; Akcea), has received conditional marketing authorization at the European Union for the treatment of familial chylomicronemia syndrome.[22] Volanesorsen is currently under review for its second attempt at obtaining FDA approval. Although not a gapmer, there is the FDA-approved nusinersen (Spinraza, Biogen) for spinal muscular atrophy treatment, an AO composed entirely of 2′-MOE nucleotides.[33,34] There are also many 2′-MOE gapmers under clinical and pre-clinical development, e.g., for Huntington's disease, amyotrophic lateral sclerosis, and Alzheimer's disease, among others.[20] Furthermore, 2′-MOE gapmers have favorable safety and pharmacokinetic profiles *in vivo*. Integrated assessments of 2′-MOE gapmer toxicity in non-human primates and human subjects found no safety concerns for liver and kidney function. Cases of thrombocytopenia and complement activation were observed; however, these were limited to animal models and not humans.[35,36] These AOs are stable *in vivo*, display broad tissue distribution, and have an elimination half-life of 2–4 weeks across tissues and species,[36] indicating the possibility of reduced patient administrations. With such a proven track record, in this study we sought to adapt the use of these 2′-MOE gapmers for the treatment of FSHD by targeting *DUX4* transcript knockdown.

We successfully demonstrated that our designed 2′-MOE gapmers could significantly reduce *DUX4* expression in immortalized

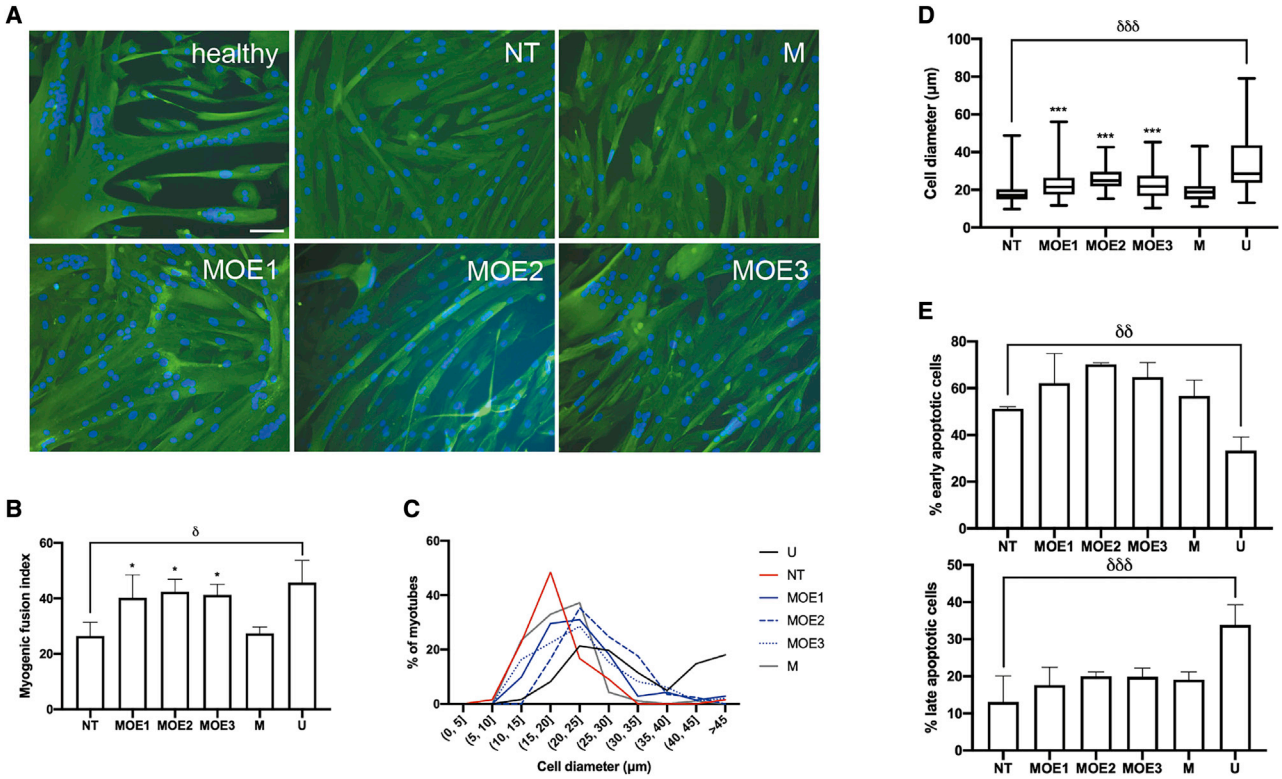

Figure 3. *In Vitro* Muscle Cell Phenotypes after 2′-MOE Gapmer Treatment

(A) Representative immunocytochemistry images of healthy immortalized control myotubes and NT, mock 2′-MOE gapmer-treated (M), and *DUX4*-specific MOE gapmer-treated (MOE1, MOE2, MOE3) immortalized FSHD patient-derived myotubes stained for nuclei (blue) and desmin (green). In this case, patient-derived myotubes were transfected with 10 nM of the various 2′-MOE gapmers at 4 days post-differentiation and then stained 3 days later. Scale bar: 100 µm. (B) Myogenic fusion index quantification for the various treatment groups. (C) Frequency distribution of myotube diameters across the different treatment groups. n = 3 independent experiments; 382 nuclei and 26 myotubes on average for each replicate, per condition, were counted for quantification of MFI and muscle cell diameters, respectively. (D) Individual myotube diameters from (C) were plotted. (E) Early and late apoptotic cell populations in immortalized FSHD patient-derived myotubes treated with 10 nM of the various 2′-MOE gapmers at 13 days post-differentiation were quantified by Annexin V/propidium iodide-based flow cytometry 1 day later. (B and E) Error bars: SD; n = 3 independent experiments. (D) The box represents the P_{25}–P_{75} with the central line marking the median, and the whiskers represent the range; n = 3. *p < 0.05, ***p < 0.0005 versus M, one-way ANOVA with Dunnett's test. $^{\delta}p < 0.05$, $^{\delta\delta}p < 0.005$, $^{\delta\delta\delta}p < 0.0005$, unpaired, two-tailed t test. See also Figure S2.

patient-derived differentiated muscle fibers (Figure 1B) and in the *FLExDUX4* FSHD mouse model (Figure 5). At the highest *in vitro* tested dose of 100 nM, we observed corresponding reductions in the expression of DUX4 downstream target genes *ZSCAN4*, *TRIM43*, and *MBD3L2* (Figure 1C). MOE3 was particularly effective among the three *DUX4*-targeting 2′-MOE gapmers. Notably, the extent of *DUX4* knockdown achieved here was comparably better than what was previously observed with PMO or 2′-OMe AOs, supporting the notion that a direct, RNase H-mediated approach to transcript knockdown is more effective at reducing gene expression than an indirect approach that relies on steric blocking AOs. We also showed that 2′-MOE treatment did not significantly reduce the expression of three out of four potential off-target genes (Figures 4B–4D). However, we did observe significantly decreased *BANF1* expression upon treatment with MOE1 and MOE2 (Figure 4A). *BANF1* codes for a DNA-binding protein with roles in cell-cycle progression, chromatin organization, and early development.[37,38] It has been reported that BANF1 is important for mouse and human embryonic stem cell (ESC) self-renewal, with BANF1 knockdown leading to their decreased survival and cloning efficiency.[38] In mouse ESCs, this also led to decreased pluripotent gene expression and increased differentiation. Because DUX4 is known to upregulate genes associated with stem cells, as well as in generating an overall less-differentiated gene expression signature in skeletal muscle,[39,40] there is the possibility that *BANF1* is a downstream DUX4 target. As such, its decreased expression may have been an indirect result of *DUX4* knockdown, but this remains to be proved.

We further confirmed the potential restorative effects of 100 nM MOE3 treatment at the transcriptomic level by RNA sequencing analysis (Figure 2). Aside from confirming the significant reduction of *ZSCAN4* and *TRIM43* expression ($p < 0.05$), we found that MOE3 treatment significantly decreased the expression of *TRIM43B*, *TRIM51*, *TRIM64B*, *PRAMEF1*, and *PRAMEF8* (Figure 2D; Figure S1; Tables S1 and S2), which belong to gene families known to be upregulated by DUX4.[14,41] We also observed a significant reduction in

Table 2. Potential Off-Target Transcripts of the 2′-MOE Gapmers, as Determined by GGGenome

Gene	Transcript Variant(s)	Sequence Showing Mismatch (5′-3′)[a]	No. of Mismatches to 2′-MOE Gapmer Target Sequence		
			MOE1	MOE2	MOE3
DUX4	N/A	CCACCTTCCGACGCTGTCTAGG	0	0	0
GALNT14	4	CCACCTTC**G**GACGCTG**A**CT-GG	3	3	3
FOXH1	N/A	CC-CCT**G**CC**C**ACGCTGTCTA**CC**	3	4	5
SSR4	1–4	CCA-CTTC**T**GACGCTGTC-A**TT**	3	4	5
ZBTB7B	1–5	**A**CACCTTCCG**CC**T**C**TCTAG**C**	4	3	4
TSPEAR-AS1	N/A	CCACCT**G**CCGA-GCTGTC-AG**C**	3	3	4
FARP1	1,3	**T**CACCTT**T**CCGA-GCTGTCT-G**T**	4	3	4
BANF1	1,2	**GT**A-CTTCCG**G**CGCTGTCT**C**GG	5	4	3

[a]Bold indicates mispairing, and underline indicates indels versus the *DUX4* target sequence.

SLC34A2 and *RFPL4B* expression, which have both been associated with FSHD;[42,43] SLC34A2 in particular has been recently reported as an FSHD protein biomarker.[43] The roles of all these genes in FSHD pathogenesis are yet to be determined, however. On another note, although DUX4 downstream target expression was reduced at the 100 nM gapmer dose, this was not the case at the 10 nM dose despite significant knockdown of *DUX4* transcript expression at this condition (Figure 1D). Increased 2′-MOE gapmer doses are recommended, because the level of *DUX4* knockdown at 10 nM may not have been sufficient to generate observable downstream effects. This once again stresses the need to achieve complete *DUX4* knockdown as much as possible, because any remaining low levels of *DUX4* expression[19] may be enough to maintain the dysregulated transcriptomic landscape seen in FSHD muscle. This scale-up of dose should be achievable *in vivo*, because 2′-MOE gapmers are non-toxic even at higher doses in humans, up to 475 mg in one study by subcutaneous or intravenous administration,[35] and a repeated dosing regimen can be easily established. We also interestingly observed increased expression of *DUX4* and its downstream target genes upon treatment with some 2′-MOE gapmers at lower doses. We are not certain why this occurs; however, this phenomenon has also been observed in a previous report that treated primary FSHD patient-derived muscle fibers with *DUX4*-targeting PMOs.[16] In that study, expression levels of the downstream target genes *ZSCAN4*, *TRIM43*, and *MBD3L2* were evaluated as well, and were found to be increased after treatment with 10 μM of certain PMOs. Because there are numerous differences between this work and ours, e.g., cell culture schedule, antisense chemistry employed, and transfection dose used, a direct comparison to identify potential reasons for this increased expression post-treatment is not possible. However, these observations provide valuable insight into considerations for future antisense therapy development, particularly concerning treatment dose, to minimize or prevent the occurrence of such off-target effects.

DUX4 orchestrates a large number of abnormal signaling events in skeletal muscle, whose cumulative effects give rise to FSHD.[14] One critically affected pathway is muscle development, with DUX4 down-regulating genes for Pax7, MyoD, and myogenin, among others.[44] As a result, FSHD myoblasts exhibit defects in fusion and differentiation, giving rise to abnormal or deformed myotube morphologies.[26,27] Treatment with *DUX4*-targeting 2′-MOE gapmers led to significant improvements in FSHD patient-derived muscle cell fusion, differentiation, and growth (Figures 3A–3D; Figure S2). In particular, treatment brought a large proportion of muscle fibers to over 20 μm in diameter, a size threshold below which characterized hypotrophic-type FSHD patient myotubes in a previous study.[26] It is interesting to note that at a 10 nM transfected 2′-MOE dose, phenotypic improvements in muscle cell morphology were observed, but not apoptosis (Figure 3E). This may be partly explained by the knowledge that DUX4 dysregulates far more pathways contributing to apoptosis than those involved in muscle development.[14] As we previously observed for low 2′-MOE gapmer doses on *in vitro* DUX4 downstream target gene expression (Figure 1D), even higher doses than those tested in this study may be required to achieve observable effects on apoptosis.

Finally, it is encouraging that we observed significant *DUX4* transcript reduction with three 20-μg i.m. injections of MOE3 in *FLExDUX4* mice (Figure 5), supporting the knockdown efficacy of our 2′-MOE gapmers not only *in vitro* but also *in vivo*. Practically, this supports the potential of i.m. injections for the muscle-specific treatment of FSHD, given how the disease exhibits asymmetric involvement of muscle groups.[1] Furthermore, this promising proof-of-concept result sets the stage for future experiments, particularly evaluation of the therapeutic efficacy of our 2′-MOE gapmers upon systemic treatment. It would be beneficial to test these gapmers in Cre-induced *FLExDUX4* mice,[24] to examine whether 2′-MOE gapmer treatment can restore DUX4-mediated downstream gene expression to normal levels and rescue FSHD phenotypes. For instance, a recent study presented that *FLExDUX4* mice crossed to *ACTA1-Mer-cre-Mer* (*ACTA1-MCM*; with a skeletal muscle-specific and tamoxifen-inducible promoter) mice produce bi-transgenic animals showing FSHD-like phenotypes, e.g., with significantly decreased skeletal muscle function.[45] Because disease severity can

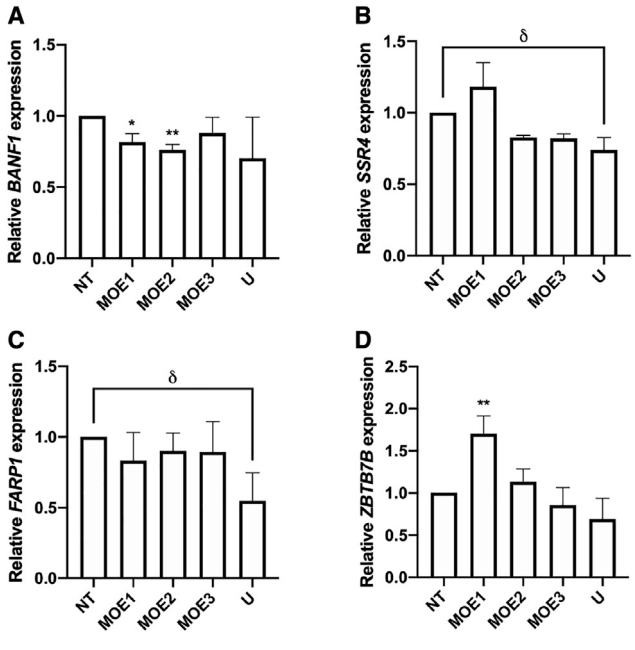

Figure 4. Off-Target Effect Evaluation upon 2′-MOE Gapmer Treatment

Immortalized patient-derived myotubes transfected with 100 nM MOE1, MOE2, or MOE3 (numbered) at 13 days post-differentiation were harvested a day later and used for quantitative real-time RT-PCR expression analysis of (A) *BANF1*, (B) *SSR4*, (C) *FARP1*, and (D) *ZBTB7B*. Error bars: SD; n = 3 independent experiments. *p < 0.05, **p < 0.005 versus NT, one-way ANOVA with Dunnett's test. $^{\delta}$p < 0.05, unpaired, two-tailed t test.

be modulated in these mice, this would be an interesting potential model for further testing of our 2′-MOE gapmers. In summary, we were able to design *DUX4*-targeting 2′-MOE gapmers that could effectively reduce *DUX4* transcript expression *in vitro* and *in vivo*, with improvements in some cellular phenotypes. Future work will evaluate the therapeutic efficacy and safety of these gapmers when administered systemically in a more severe FSHD animal model, to further assess their potential as candidate FSHD therapeutics.

MATERIALS AND METHODS

AOs and Cell Culture

Experiments involving human cells were approved by the Health Research Ethics Board at University of Alberta. Our group designed three 2′-MOE gapmers (MOE1–3) with target sequences on *DUX4* exon 3, before the PAS (Figure 1A). Target sites were chosen based on GC content and the mRNA secondary structure at the region. All gapmers were 20 bp long, fully phosphorothioated, consisted of a central 10-bp DNA segment flanked by 5 bp of 2′-MOE-modified nucleotides on each side, and synthesized by Eurogentec (Belgium). Gapmer sequences and characteristics are summarized in Table 1.

Cell culture was performed using immortalized WS229 FSHD patient-derived and WS234 healthy control myoblasts obtained in kind from the University of Massachusetts Medical School (MA, USA) Wellstone Program. Cells were derived from biceps biopsies of siblings and immortalized via stable *CDK4*/*hTERT* cassette integration[46] (Table S3). For growing cells, a growth medium was prepared with 15% fetal bovine serum (FBS) (Sigma, St. Louis, MO, USA), 0.055 μg/mL dexamethasone, 2.5 ng/mL recombinant human hepatocyte growth factor (EMD Millipore, Burlington, MA, USA), and 10 ng/mL recombinant human fibroblast growth factor (BioPioneer, San Diego, CA, USA) in basal medium (BM; 20% Medium 199 [Life Technologies, Carlsbad, CA, USA], 0.03 μg/mL $ZnSO_4$, 1.4 μg/mL vitamin B_{12}, and 2.5% penicillin-streptomycin in DMEM [Life Technologies]). For differentiation, the following was prepared: 15% KnockOut Serum Replacement (KOSR; Life Technologies),[47] 10 μg/mL insulin (Sigma), and 100 μg/mL human apo-transferrin (R&D Systems, Minneapolis, MN, USA) in BM. All cells were cultured at 37°C and 5% CO_2.

Transfection for Gapmer Screen

For AO transfection, 4×10^5 WS229 or WS234 cells/well were seeded onto six-well plates and differentiated the following day. Gapmers against *DUX4* or a mock 2′-MOE gapmer were prepared at 100, 10, and 1 nM doses in 2% Lipofectamine RNAiMAX (Life Technologies) in OptiMEM (Life Technologies) following the manufacturer's instructions. The transfection mixture was then diluted with differentiation medium at a 1:5 ratio, after which the final mixture was given to WS229 cells at 13 days post-differentiation. WS229 cells were also subjected to transfection but without any gapmer as non-treated control. Cells were transfected overnight and harvested the following day.

RNA Extraction and Quantitative Real-Time RT-PCR

Total cell RNA extracts were obtained using the RNeasy Mini Kit (-QIAGEN, Germany) with on-column DNase treatment, following the manufacturer's instructions. For cDNA synthesis, SuperScript IV Reverse Transcriptase (Life Technologies) was used following the manufacturer's instructions with 1,400 ng RNA extract and 0.5 μg oligo(dT)$_{12–18}$ primer (Life Technologies). Using this cDNA, we then performed quantitative real-time RT-PCR with the QuantStudio 3 Real-Time PCR system (Applied Biosystems, Foster City, CA, USA) to evaluate transcript expression of the following genes: *DUX4*, *GAPDH*, *ZSCAN4*, *TRIM43*, *MBD3L2*, *TRIM48*, *TRIM64B*, *PRAMEF4/5/9/11*, *BANF1*, *SSR4*, *FARP1*, and *ZBTB7B*. Probe-based TaqMan Gene Expression assays (Thermo Fisher, Waltham, MA, USA; reference numbers in parentheses) with the TaqMan Fast Advanced Master Mix (Thermo Fisher) were used for *ZSCAN4* (Hs00537549_m1), *TRIM43* (Hs00299174_m1), *MBD3L2* (Hs00544743_m1), and *TRIM64B* (Hs04194067_mH) expression analysis. For the other genes, a SYBR-based system was used, with SsoAdvanced Universal SYBR Green Supermix (Bio-Rad, Hercules, CA, USA). Primers were designed for these genes and are listed in Table S4. The default Fast cycling program corresponding to the detection system was used for quantitative real-time RT-PCR: (1) 95°C, 20 s; and (2) 40 cycles of 95°C, 1 s and then 60°C, 20 s. Expression levels were normalized to those of *GAPDH* and determined using the ΔΔCt method.

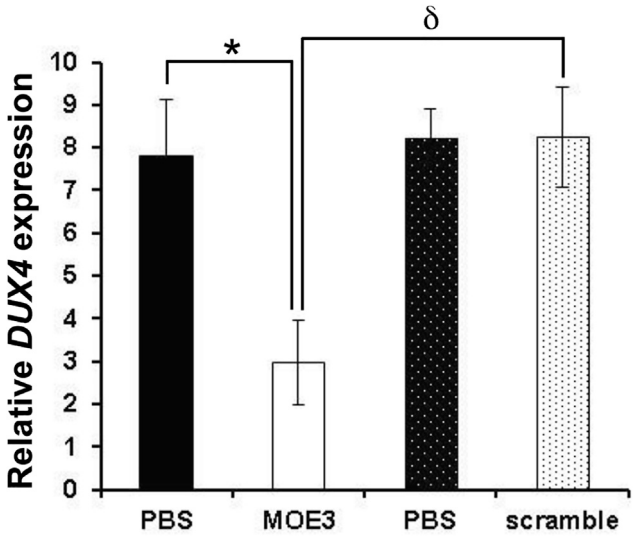

Figure 5. *In Vivo* Efficacy of MOE3 Gapmer Treatment in *FLExDUX4* Mice
Intramuscular injections of 20 μg MOE3 to the TA muscles (one leg with MOE3 and the contralateral leg with PBS) every other day for a total of three injections showed knockdown of *DUX4* mRNA by quantitative real-time RT-PCR 1 day after the last injection. No knockdown was observed when a 2′-MOE gapmer control with a scrambled sequence was injected instead. Bars with similar patterns (block or hashed) indicate leg pairs. Error bars: SEM; n = 5 for MOE3/PBS mice and n = 3 for scrambled 2′-MOE/PBS mice. *$p < 0.05$, paired, two-tailed t test. $^{\delta}p < 0.05$, unpaired, two-tailed t test.

RNA Sequencing and Bioinformatics

Total RNA was extracted from WS234, non-treated WS229 myotubes, and MOE3-treated WS229 myotubes as described in RNA Extraction and Quantitative Real-Time RT-PCR. WS229 myotubes were treated with the MOE3 gapmer as in Transfection for Gapmer Screen. RNA quality was determined using an Agilent 2000 bioanalyzer instrument (Agilent, Santa Clara, CA, USA) and a high-sensitivity RNA chip (Agilent). Total RNA was quantified using Qubit 2.0 and an RNA high-sensitivity Assay Kit (Invitrogen, Carlsbad, CA, USA). RNA sequencing (RNA-seq) libraries were constructed from 100 ng total RNA with the NEBNext Ultra II Directional RNA Library Prep Kit for Illumina (NEB, Ipswich, MA, USA), according to the manufacturer's instructions. In brief, polyadenylated mRNA was enriched with dT oligos conjugated to paramagnetic beads. Enriched mRNA was chemically fragmented, end repaired, A tailed, and ligated to sequencing linkers. Linker sequences were used as binding sites to incorporate indexed sequencing adapters by 12 cycles of PCR. Libraries were inspected using a High-Sensitivity DNA bioanalyzer chip (Agilent), and the DNA was quantified using a High-Sensitivity DNA Qubit assay (Invitrogen). Indexed libraries were pooled to a final concentration of 4 nM and were finally sequenced at a 10 pM concentration using a MiSeq instrument (Illumina, San Diego, CA, USA), with a 75-cycle paired-end protocol that included on-instrument de-multiplexing.

Sequences were inspected with fastqc, and bases with quality (Q) scores lower than 30 were trimmed with fastq-mcf. Pseudo-alignment of sequences against the GRCH38 version of the human cDNA database from the Ensembl database was conducted with Kallisto, using 100 bootstraps and bias correction.[48] Transcripts that accumulated an average of at least 10 reads were subjected to statistical analysis. Differential expression analysis of RNA-seq data was conducted using negative binomial generalized linear models with the DESeq2 R package.[49] Plots were generated with in-house R scripts. RNA sequencing datasets are available at the NCBI SRA: PRJNA629563.

Cellular Phenotype Analysis

For immunocytochemistry, WS229 cells in 24-well plates seeded at 2.5×10^4 cells/well were transfected as indicated in Transfection for Gapmer Screen with 10 nM 2′-MOE gapmers at 4 days post-differentiation (overnight transfection). Cells at 7 days post-differentiation or 3 days post-transfection were fixed for 5 min with 4% paraformaldehyde, incubated for 5 min with 0.5% Triton X-100 in PBS, and blocked for 1 h with 20% FBS in PBS. Cells were then stained for desmin (1:200 rabbit polyclonal antibody [Abcam, UK] for 1 h, followed by three 5-min PBS washes, and then 1:100 Alexa 594 goat anti-rabbit IgG [H+L] [Life Technologies]), given three final 5-min PBS washes, and mounted with SlowFade Gold Antifade Mountant with DAPI (Life Technologies). The Nikon Eclipse TE 2000-U fluorescence microscope was used for visualization. MFI determination and cell diameter measurements were done blinded using ImageJ (NIH), from three randomly chosen fields of view for each replicate, per condition. For MFI calculation, the number of nuclei in myotubes was divided by the total number of nuclei in a given field of view and then multiplied by 100 to get a percentage value. Approximately 382 nuclei on average were counted per replicate, per condition (range: 69–541). Myotube diameters were taken as the average of the three widest measurements across the length of a myotube, avoiding locations near branch points or overlaps between myotubes. Approximately 26 myotubes on average were counted per replicate, per condition (range: 15–36). For purposes of quantification, we considered a myotube as a cell with at least two nuclei having the same cytoplasm. For apoptosis analysis, WS229 cells in 24-well plates seeded at 5×10^4 cells/well were transfected as above with 10 nM 2′-MOE gapmers at 13 days post-differentiation. Apoptosis was then assessed by flow cytometry with the eBioscience Annexin V Apoptosis Detection Kit FITC (Thermo Fisher). WS234 cells were grown alongside WS229 cells and subjected to similar procedures to serve as a control.

Western Blotting

WS229 and WS234 cells were seeded and differentiated in six-well plates as described in AOs and Cell Culture. Transfection with 100 nM of either MOE1, MOE2, MOE3, or mock 2′-MOE gapmers to WS229 myotubes was done as in Transfection for Gapmer Screen, with transfection performed at 4 days post-differentiation (overnight). Total protein was extracted from cells at 7 days post-differentiation or 3 days post-transfection using radioimmunoprecipitation assay (RIPA) buffer (Sigma) with cOmplete, Mini, EDTA-free protease inhibitor cocktail (Sigma); protein was quantified using the Pierce BCA Protein Assay kit (Thermo Fisher). For SDS-PAGE, 12 μg of protein extracts was loaded and run on a NuPAGE 4%–12% Bis-

Tris gel (Thermo Fisher) at 150 V for 70 min. Semi-dry transfer onto a polyvinylidene fluoride (PVDF) membrane (Millipore) was then performed at 20 V for 30 min. Blocking was done overnight at 4°C using 5% skim milk in PBS with 0.05% Tween 20 (PBST). The next day, the membrane was cut and incubated in primary antibodies against myosin heavy chain (MF20, 1:800 in blocking solution; Developmental Studies Hybridoma Bank, Iowa City, IA, USA) or β-tubulin (ab6046, 1:5,000 in PBST; Abcam) for 1 h at room temperature, followed by three 10-min PBST washes. Membranes were then incubated in 1:10,000 of the corresponding HRP-conjugated secondary antibody (anti-mouse IgG H+L for the myosin heavy chain antibody, and anti-rabbit IgG H+L for the β-tubulin antibody; Invitrogen) in PBST for 1 h at room temperature, followed again by three 10-min PBST washes. Bands were visualized using the Amersham ECL Select detection kit (GE Healthcare, Chicago, IL, USA). Myosin heavy chain protein levels were determined based on band intensities normalized to those of β-tubulin and calculated relative to the normalized band intensity of one of the three WS234 replicates.

Searching for Potential Off-Target Genes

The GGGenome search engine (https://gggenome.dbcls.jp/) was used to find targets with highly similar sequences to those recognized by the various *DUX4*-targeting 2′-MOE gapmers.[50] The RefSeq human RNA release 80 (Jan 2017) database was used for the search. The top hits are shown in Table S4. Only *BANF1*, *SSR4*, *FARP1*, and *ZBTB7B* were found to have detectable expression by quantitative real-time RT-PCR in our *in vitro* system, and so we focused on these for off-target analysis.

In Vivo Delivery of 2′-MOE Gapmers

Experiments involving animals were approved by the Institutional Animal Care and Use Committee at the Children's National Health System, Washington, DC, USA. The animal experiment was also approved by the University of Alberta. To examine the effect of 2′-MOE gapmer treatment on *DUX4* expression, five adult hemizygous *FLExDUX4* mice (three male, two female; 2–3 months old) received three i.m. injections of MOE3 (20 μg dissolved in PBS, for a final 20 μL volume) to the TA muscle over 6 days, one injection every other day. The contralateral TA of each mouse was injected with PBS (20 μL) as a control. In addition, three adult male hemizygous *FLExDUX4* mice were similarly injected i.m. (TA) with a scrambled 2′-MOE gapmer control following the same dose and treatment schedule; contralateral TAs were injected with PBS as before. Twenty-four hours after the final injection, mice were euthanized by CO_2 asphyxiation with cervical dislocation, and TAs were dissected, cleaned of connective tissue, snap frozen in dry ice-cooled isopentane, and stored at −80°C for further analysis. For *DUX4* expression analysis, quantitative real-time RT-PCR was performed as previously described.[47,51] In brief, RNA was extracted using TRIzol (Ambion, Austin, TX, USA) and cleaned up using the RNeasy Plus Mini Kit (QIAGEN). cDNA was synthesized from 2 μg of total RNA using SuperScript IV Reverse Transcriptase (Life Technologies) and oligo$(dT)_{12–18}$ primers. *Gapdh* was used as an internal control, and relative gene expression was analyzed using the ΔΔCt method.

Statistical Analysis

Statistical analyses for all data besides those from RNA sequencing were done with GraphPad Prism 7 (GraphPad Software). One-way ANOVAs with post hoc Tukey's or Dunnett's test, or unpaired two-tailed t tests were used as needed.

SUPPLEMENTAL INFORMATION

Supplemental Information can be found online at https://doi.org/10.1016/j.ymthe.2020.10.010.

AUTHOR CONTRIBUTIONS

K.R.Q.L., Y.-W.C., and T.Y. conceived and designed the study. Y.-W.C. and T.Y. supervised the work. K.R.Q.L., R.M., and Y.E. designed the gapmers. K.R.Q.L., A.B., Q.N., Y.H., K.D., and A.Z. performed the experiments. K.R.Q.L., A.B., Y.-W.C., and T.Y. wrote the manuscript.

CONFLICTS OF INTEREST

The authors declare no competing interests.

ACKNOWLEDGMENTS

We would like to thank Dr. Juan Jovel and The Applied Genomics Core (University of Alberta), as well as Dr. Aja Rieger and the Flow Cytometry Facility (University of Alberta), for their excellent advice and technical assistance toward this study. This work was supported by the FSH Society (grants 82018-2 and 82016-4), Muscular Dystrophy Canada (grant 82016-4), University of Alberta, Women and Children's Health Research Institute Graduate Studentship award and Innovation Grant (2874), Alberta Innovates Graduate Studentship Award (201810476), Friends of FSH Research (grant 20170528), FSHD Global Research Foundation (34), FSHD Canada Foundation, The Friends of Garrett Cumming Research Fund, HM Toupin Neurological Science Research Fund, Canadian Institutes of Health Research (grant 143251), Canada Foundation for Innovation (grant 30819), Alberta Enterprise and Advanced Education, University Hospital Foundation, National Institutes of Health, Muscular Dystrophy Association—Strength, Science, and Stories of Inspiration Fellowship, and the FSHD Society New Investigator Grant Award.

REFERENCES

1. Wang, L.H., and Tawil, R. (2016). Facioscapulohumeral Dystrophy. Curr. Neurol. Neurosci. Rep. *16*, 66.

2. Deenen, J.C.W., Arnts, H., van der Maarel, S.M., Padberg, G.W., Verschuuren, J.J.G.M., Bakker, E., Weinreich, S.S., Verbeek, A.L., and van Engelen, B.G. (2014). Population-based incidence and prevalence of facioscapulohumeral dystrophy. Neurology *83*, 1056–1059.

3. Richards, M., Coppée, F., Thomas, N., Belayew, A., and Upadhyaya, M. (2012). Facioscapulohumeral muscular dystrophy (FSHD): an enigma unravelled? Hum. Genet. *131*, 325–340.

4. Klinge, L., Eagle, M., Haggerty, I.D., Roberts, C.E., Straub, V., and Bushby, K.M. (2006). Severe phenotype in infantile facioscapulohumeral muscular dystrophy. Neuromuscul. Disord. *16*, 553–558.

5. Brouwer, O.F., Padberg, G.W., Wijmenga, C., and Frants, R.R. (1994). Facioscapulohumeral muscular dystrophy in early childhood. Arch. Neurol. *51*, 387–394.

6. Goselink, R.J.M., Voermans, N.C., Okkersen, K., Brouwer, O.F., Padberg, G.W., Nikolic, A., Tupler, R., Dorobek, M., Mah, J.K., van Engelen, B.G.M., et al. (2017).

Early onset facioscapulohumeral dystrophy—a systematic review using individual patient data. Neuromuscul. Disord. *27*, 1077–1083.

7. Lu, J., Yao, Z., Yang, Y., Zhang, C., Zhang, J., and Zhang, Y. (2019). Management strategies in facioscapulohumeral muscular dystrophy. Intractable Rare Dis. Res. *8*, 9–13.
8. Gabriëls, J., Beckers, M.C., Ding, H., De Vriese, A., Plaisance, S., van der Maarel, S.M., Padberg, G.W., Frants, R.R., Hewitt, J.E., Collen, D., and Belayew, A. (1999). Nucleotide sequence of the partially deleted D4Z4 locus in a patient with FSHD identifies a putative gene within each 3.3 kb element. Gene *236*, 25–32.
9. Lemmers, R.J.L.F., van der Vliet, P.J., Klooster, R., Sacconi, S., Camaño, P., Dauwerse, J.G., Snider, L., Straasheijm, K.R., van Ommen, G.J., Padberg, G.W., et al. (2010). A unifying genetic model for facioscapulohumeral muscular dystrophy. Science *329*, 1650–1653.
10. Hewitt, J.E., Lyle, R., Clark, L.N., Valleley, E.M., Wright, T.J., Wijmenga, C., van Deutekom, J.C., Francis, F., Sharpe, P.T., Hofker, M., et al. (1994). Analysis of the tandem repeat locus D4Z4 associated with facioscapulohumeral muscular dystrophy. Hum. Mol. Genet. *3*, 1287–1295.
11. Hewitt, J.E. (2015). Loss of epigenetic silencing of the DUX4 transcription factor gene in facioscapulohumeral muscular dystrophy. Hum. Mol. Genet. *24* (R1), R17–R23.
12. Lemmers, R.J.L.F., Goeman, J.J., van der Vliet, P.J., van Nieuwenhuizen, M.P., Balog, J., Vos-Versteeg, M., Camano, P., Ramos Arroyo, M.A., Jerico, I., Rogers, M.T., et al. (2015). Inter-individual differences in CpG methylation at D4Z4 correlate with clinical variability in FSHD1 and FSHD2. Hum. Mol. Genet. *24*, 659–669.
13. Himeda, C.L., and Jones, P.L. (2019). The Genetics and Epigenetics of Facioscapulohumeral Muscular Dystrophy. Annu. Rev. Genomics Hum. Genet. *20*, 265–291.
14. Lim, K.R.Q., Nguyen, Q., and Yokota, T. (2020). DUX4 Signalling in the Pathogenesis of Facioscapulohumeral Muscular Dystrophy. Int. J. Mol. Sci. *21*, 729.
15. Marsollier, A.-C., Ciszewski, L., Mariot, V., Popplewell, L., Voit, T., Dickson, G., and Dumonceaux, J. (2016). Antisense targeting of 3′ end elements involved in DUX4 mRNA processing is an efficient therapeutic strategy for facioscapulohumeral dystrophy: a new gene-silencing approach. Hum. Mol. Genet. *25*, 1468–1478.
16. Chen, J.C., King, O.D., Zhang, Y., Clayton, N.P., Spencer, C., Wentworth, B.M., Emerson, C.P., Jr., and Wagner, K.R. (2016). Morpholino-mediated Knockdown of DUX4 Toward Facioscapulohumeral Muscular Dystrophy Therapeutics. Mol. Ther. *24*, 1405–1411.
17. Ansseau, E., Vanderplanck, C., Wauters, A., Harper, S.Q., Coppée, F., and Belayew, A. (2017). Antisense Oligonucleotides Used to Target the DUX4 mRNA as Therapeutic Approaches in FaciosScapuloHumeral Muscular Dystrophy (FSHD). Genes (Basel) *8*, 93.
18. Vanderplanck, C., Ansseau, E., Charron, S., Stricwant, N., Tassin, A., Laoudj-Chenivesse, D., Wilton, S.D., Coppée, F., and Belayew, A. (2011). The FSHD atrophic myotube phenotype is caused by DUX4 expression. PLoS One *6*, e26820.
19. Tassin, A., Laoudj-Chenivesse, D., Vanderplanck, C., Barro, M., Charron, S., Ansseau, E., Chen, Y.W., Mercier, J., Coppée, F., and Belayew, A. (2013). DUX4 expression in FSHD muscle cells: how could such a rare protein cause a myopathy? J. Cell. Mol. Med. *17*, 76–89.
20. Scoles, D.R., Minikel, E.V., and Pulst, S.M. (2019). Antisense oligonucleotides: A primer. Neurol. Genet. *5*, e323.
21. Shen, X., and Corey, D.R. (2018). Chemistry, mechanism and clinical status of antisense oligonucleotides and duplex RNAs. Nucleic Acids Res. *46*, 1584–1600.
22. Paik, J., and Duggan, S. (2019). Volanesorsen: First Global Approval. Drugs *79*, 1349–1354.
23. Khvorova, A., and Watts, J.K. (2017). The chemical evolution of oligonucleotide therapies of clinical utility. Nat. Biotechnol. *35*, 238–248.
24. Jones, T., and Jones, P.L. (2018). A cre-inducible DUX4 transgenic mouse model for investigating facioscapulohumeral muscular dystrophy. PLoS One *13*, e0192657.
25. Rickard, A.M., Petek, L.M., and Miller, D.G. (2015). Endogenous DUX4 expression in FSHD myotubes is sufficient to cause cell death and disrupts RNA splicing and cell migration pathways. Hum. Mol. Genet. *24*, 5901–5914.
26. Barro, M., Carnac, G., Flavier, S., Mercier, J., Vassetzky, Y., and Laoudj-Chenivesse, D. (2010). Myoblasts from affected and non-affected FSHD muscles exhibit morphological differentiation defects. J. Cell. Mol. Med. *14*, 275–289.
27. Banerji, C.R.S., Panamarova, M., Pruller, J., Figeac, N., Hebaishi, H., Fidanis, E., Saxena, A., Contet, J., Sacconi, S., Severini, S., and Zammit, P.S. (2019). Dynamic transcriptomic analysis reveals suppression of PGC1α/ERRα drives perturbed myogenesis in facioscapulohumeral muscular dystrophy. Hum. Mol. Genet. *28*, 1244–1259.
28. Kowaljow, V., Marcowycz, A., Ansseau, E., Conde, C.B., Sauvage, S., Mattéotti, C., Arias, C., Corona, E.D., Nuñez, N.G., Leo, O., et al. (2007). The DUX4 gene at the FSHD1A locus encodes a pro-apoptotic protein. Neuromuscul. Disord. *17*, 611–623.
29. Garay, M., Gaarde, W., Monia, B.P., Nero, P., and Cioffi, C.L. (2000). Inhibition of hypoxia/reoxygenation-induced apoptosis by an antisense oligonucleotide targeted to JNK1 in human kidney cells. Biochem. Pharmacol. *59*, 1033–1043.
30. Levesque, L., Dean, N.M., Sasmor, H., and Crooke, S.T. (1997). Antisense oligonucleotides targeting human protein kinase C-alpha inhibit phorbol ester-induced reduction of bradykinin-evoked calcium mobilization in A549 cells. Mol. Pharmacol. *51*, 209–216.
31. Geary, R.S., Baker, B.F., and Crooke, S.T. (2015). Clinical and preclinical pharmacokinetics and pharmacodynamics of mipomersen (kynamro(®)): a second-generation antisense oligonucleotide inhibitor of apolipoprotein B. Clin. Pharmacokinet. *54*, 133–146.
32. Keam, S.J. (2018). Inotersen: First Global Approval. Drugs *78*, 1371–1376.
33. Meijboom, K.E., Wood, M.J.A., and McClorey, G. (2017). Splice-Switching Therapy for Spinal Muscular Atrophy. Genes (Basel) *8*, 161.
34. Goodkey, K., Aslesh, T., Maruyama, R., and Yokota, T. (2018). Nusinersen in the treatment of spinal muscular atrophy. In Exon Skipping and Inclusion Therapies, *1828*, T. Yokota and R. Maruyama, eds (NY: Humana Press), pp. 69–76.
35. Crooke, S.T., Baker, B.F., Kwoh, T.J., Cheng, W., Schulz, D.J., Xia, S., Salgado, N., Bui, H.H., Hart, C.E., Burel, S.A., et al. (2016). Integrated Safety Assessment of 2′-O-Methoxyethyl Chimeric Antisense Oligonucleotides in NonHuman Primates and Healthy Human Volunteers. Mol. Ther. *24*, 1771–1782.
36. Crooke, S.T., Baker, B.F., Xia, S., Yu, R.Z., Viney, N.J., Wang, Y., Tsimikas, S., and Geary, R.S. (2019). Integrated Assessment of the Clinical Performance of $GalNAc_3$-Conjugated 2′-O-Methoxyethyl Chimeric Antisense Oligonucleotides: I. Human Volunteer Experience. Nucleic Acid Ther. *29*, 16–32.
37. Margalit, A., Brachner, A., Gotzmann, J., Foisner, R., and Gruenbaum, Y. (2007). Barrier-to-autointegration factor—a BAFfling little protein. Trends Cell Biol. *17*, 202–208.
38. Cox, J.L., Mallanna, S.K., Ormsbee, B.D., Desler, M., Wiebe, M.S., and Rizzino, A. (2011). Banf1 is required to maintain the self-renewal of both mouse and human embryonic stem cells. J. Cell Sci. *124*, 2654–2665.
39. Knopp, P., Krom, Y.D., Banerji, C.R.S., Panamarova, M., Moyle, L.A., den Hamer, B., van der Maarel, S.M., and Zammit, P.S. (2016). DUX4 induces a transcriptome more characteristic of a less-differentiated cell state and inhibits myogenesis. J. Cell Sci. *129*, 3816–3831.
40. Geng, L.N., Yao, Z., Snider, L., Fong, A.P., Cech, J.N., Young, J.M., van der Maarel, S.M., Ruzzo, W.L., Gentleman, R.C., Tawil, R., and Tapscott, S.J. (2012). DUX4 activates germline genes, retroelements, and immune mediators: implications for facioscapulohumeral dystrophy. Dev. Cell *22*, 38–51.
41. Yao, Z., Snider, L., Balog, J., Lemmers, R.J.L.F., Van Der Maarel, S.M., Tawil, R., and Tapscott, S.J. (2014). DUX4-induced gene expression is the major molecular signature in FSHD skeletal muscle. Hum. Mol. Genet. *23*, 5342–5352.
42. Banerji, C.R.S., Panamarova, M., Hebaishi, H., White, R.B., Relaix, F., Severini, S., and Zammit, P.S. (2017). PAX7 target genes are globally repressed in facioscapulohumeral muscular dystrophy skeletal muscle. Nat. Commun. *8*, 2152.
43. Mueller, A.L., O'Neill, A., Jones, T.I., Llach, A., Rojas, L.A., Sakellariou, P., Stadler, G., Wright, W.E., Eyerman, D., Jones, P.L., and Bloch, R.J. (2019). Muscle xenografts reproduce key molecular features of facioscapulohumeral muscular dystrophy. Exp. Neurol. *320*, 113011.
44. Bosnakovski, D., Xu, Z., Gang, E.J., Galindo, C.L., Liu, M., Simsek, T., Garner, H.R., Agha-Mohammadi, S., Tassin, A., Coppée, F., et al. (2008). An isogenetic myoblast expression screen identifies DUX4-mediated FSHD-associated molecular pathologies. EMBO J. *27*, 2766–2779.

45. Jones, T.I., Chew, G.-L., Barraza-Flores, P., Schreier, S., Ramirez, M., Wuebbles, R.D., Burkin, D.J., Bradley, R.K., and Jones, P.L. (2020). Transgenic mice expressing tunable levels of DUX4 develop characteristic facioscapulohumeral muscular dystrophy-like pathophysiology ranging in severity. Skelet. Muscle *10*, 8.

46. Stadler, G., Chen, J.C.J., Wagner, K., Robin, J.D., Shay, J.W., Emerson, C.P., Jr., and Wright, W.E. (2011). Establishment of clonal myogenic cell lines from severely affected dystrophic muscles - CDK4 maintains the myogenic population. Skelet. Muscle *1*, 12.

47. Pandey, S.N., Khawaja, H., and Chen, Y.-W. (2015). Culture Conditions Affect Expression of DUX4 in FSHD Myoblasts. Molecules *20*, 8304–8315.

48. Bray, N.L., Pimentel, H., Melsted, P., and Pachter, L. (2016). Near-optimal probabilistic RNA-seq quantification. Nat. Biotechnol. *34*, 525–527.

49. Love, M.I., Huber, W., and Anders, S. (2014). Moderated estimation of fold change and dispersion for RNA-seq data with DESeq2. Genome Biol. *15*, 550.

50. Yoshida, T., Naito, Y., Sasaki, K., Uchida, E., Sato, Y., Naito, M., Kawanishi, T., Obika, S., and Inoue, T. (2018). Estimated number of off-target candidate sites for antisense oligonucleotides in human mRNA sequences. Genes Cells *23*, 448–455.

51. Pandey, S.N., Cabotage, J., Shi, R., Dixit, M., Sutherland, M., Liu, J., Muger, S., Harper, S.Q., Nagaraju, K., and Chen, Y.W. (2012). Conditional over-expression of PITX1 causes skeletal muscle dystrophy in mice. Biol. Open *1*, 629–639.

YMTHE, Volume *29*

Supplemental Information

DUX4 Transcript Knockdown with Antisense 2′-*O*-Methoxyethyl Gapmers for the Treatment of Facioscapulohumeral Muscular Dystrophy

Kenji Rowel Q. Lim, Adam Bittel, Rika Maruyama, Yusuke Echigoya, Quynh Nguyen, Yiqing Huang, Kasia Dzierlega, Aiping Zhang, Yi-Wen Chen, and Toshifumi Yokota

Supplemental Information

Supplemental Figures

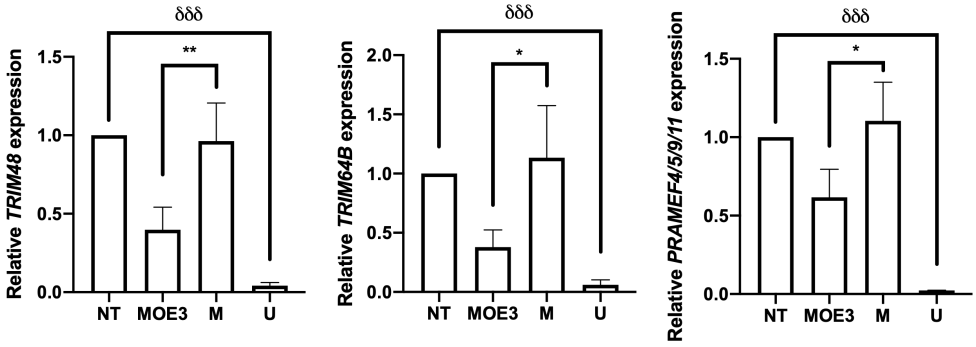

Figure S1. qPCR analysis of *TRIM48*, *TRIM64B*, and *PRAMEF4/5/9/11* expression (see also Figure 2). Relative expression levels of *TRIM48*, *TRIM64B*, and *PRAMEF4/5/9/11*, all significantly up-regulated FSHD-associated genes identified from our RNA sequencing analysis, were found to be significantly reduced by MOE3 treatment compared to mock gapmer-treated (M) controls. NT, non-treated; U, FSHD-unaffected/healthy. Error bars: S.D., n=3. *p<0.05, **p<0.005 vs M, one-way ANOVA with Dunnett's test. δδδ p<0.0005, unpaired, two-tailed t-test.

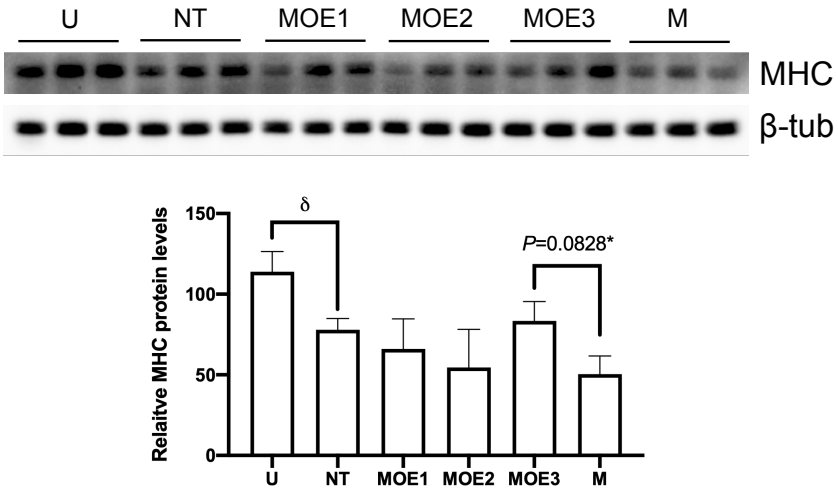

Figure S2. Western blot analysis of myosin heavy chain protein levels (see also Figure 3). Myosin heavy chain (MHC) protein levels were detected via Western blot, with β-tubulin (β-tub) as the loading control. Protein samples (12 µg) were extracted from healthy WS234 myotubes (U), non-treated FSHD WS229 myotubes (NT), 2'-MOE gapmer-treated WS229 myotubes (MOE1-MOE3), and mock 2'-MOE gapmer-treated WS229 myotubes (M). Top: image of the visualized Western blot, bottom: quantification of MHC protein levels normalized to β-tub and calculated relative to one replicate from the healthy myotube samples. Error bars: S.D., n=3. *one-way ANOVA with Dunnett's test vs M. δ $p<0.05$, unpaired, two-tailed *t*-test.

Supplemental Tables

Table S1. Information on the 94 FSHD signature genes obtained from RNA sequencing analysis.

Gene*	Transcript ID	Non-treated FSHD vs Healthy**			Treated FSHD vs Non-treated FSHD**		
		log2FC	adj. p-value	up/down?	log2FC	adj. p-value	significantly restored by treatment?
HSPA1B_a	ENST00000391555	12.81	1.60E-25	up	0.18	0.05558362	No
MBD3L3	ENST00000333843	10.23	6.80E-16	up	-0.66	0.150525844	No
PSMB9_a	ENST00000453059	8.16	1.31E-09	up	-0.79	0.320090145	No
PSMB9_b	ENST00000434471	8.16	1.31E-09	up	-0.79	0.320090145	No
PSMB9_c	ENST00000427870	8.16	1.31E-09	up	-0.79	0.320090145	No
TRIM51	ENST00000449290	7.89	6.11E-09	up	-1.18	0.036749033	Yes
KDM4E	ENST00000450979	7.61	2.42E-08	up	-0.51	0.670007042	No
PRAMEF17	ENST00000376098	7.59	4.53E-08	up	-0.12	0.990219585	No
PFKFB3	ENST00000536985	7.58	4.68E-07	up	-2.63	0.58814826	No
AMOT_a	ENST00000371959	7.38	2.26E-06	up	-0.13	0.992445062	No
PRAMEF9	ENST00000415919	7.38	6.87E-07	up	-1.12	0.457011498	No
TFIP11	ENST00000619735	7.37	0.011892526	up	0.49	0.983196789	No
STIL_a	ENST00000337817	7.30	0.012435153	up	-0.61	0.982576204	No
KHDC1L_a	ENST00000471312	7.12	8.45E-07	up	0.48	0.781306098	No
ZNF280A_a	ENST00000302097	7.09	6.64E-07	up	-0.05	0.995731523	No
ZNF280A_b	ENST00000620282	7.09	6.64E-07	up	-0.05	0.995731523	No
PRAMEF10	ENST00000235347	6.87	4.31E-06	up	-0.36	0.943642771	No
AMACR	ENST00000506639	6.71	0.034837731	up	-0.85	0.978289808	No
KHDC1L_b	ENST00000370388	6.48	3.58E-29	up	-0.20	0.821838147	No
LEUTX_a	ENST00000396841	6.36	1.06E-07	up	-0.65	0.30504829	No
LEUTX_b	ENST00000629267	6.36	1.06E-07	up	-0.65	0.30504829	No
PRAMEF22	ENST00000616664	6.36	3.43E-05	up	0.14	0.991303373	No
AMOT_b	ENST00000304758	6.21	6.02E-05	up	0.18	0.987440238	No
TRIM43	ENST00000272395	6.19	1.02E-15	up	-1.31	0.00068713	Yes
PRAMEF4	ENST00000235349	6.05	2.74E-05	up	-0.50	0.768132302	No
TRIM48	ENST00000417545	5.96	0.000173991	up	-1.72	0.249308715	No
SLC34A2_a	ENST00000382051	5.88	4.53E-17	up	-0.73	3.34E-05	Yes
ZSCAN4	ENST00000612521	5.86	5.07E-16	up	-1.15	0.00014191	Yes
PRAMEF2	ENST00000240189	5.76	1.04E-06	up	-1.52	0.133552181	No
SLC34A2_b	ENST00000513204	5.75	3.45E-06	up	-0.44	0.747265402	No
PRAMEF19	ENST00000376101	5.60	0.000249056	up	0.25	0.982576204	No
PRAMEF5_a	ENST00000622421	5.45	1.85E-08	up	-0.73	0.475006079	No
PRAMEF5_b	ENST00000621481	5.45	1.85E-08	up	-0.73	0.475006079	No
PRAMEF1	ENST00000332296	5.36	1.14E-07	up	-1.51	8.51E-05	Yes
TRIM43B	ENST00000432468	5.28	3.97E-11	up	-1.64	0.001063378	Yes
PRAMEF12	ENST00000357726	5.26	5.65E-07	up	-0.80	0.345957318	No
MBD3L2	ENST00000381393	5.21	4.98E-10	up	-0.37	0.576811781	No

Table S1 (cont'd.)

Gene*	Transcript ID	Non-treated FSHD vs Healthy**			Treated FSHD vs Non-treated FSHD**		
		log2FC	adj. p-value	up/down?	log2FC	adj. p-value	significantly restored by treatment?
TRIM49C	ENST00000448984	5.21	0.000369479	up	-0.56	0.876161011	No
THOC5_a	ENST00000488052	5.18	8.26E-07	up	-0.69	0.495486875	No
OLFM1	ENST00000252854	4.81	8.15E-05	up	0.12	0.988946093	No
HSPA1B_b	ENST00000391548	4.78	4.55E-70	up	-0.02	0.991152883	No
TRIM49	ENST00000329758	4.78	0.000403045	up	-1.55	0.187848853	No
TRIM49B	ENST00000332682	4.56	1.13E-07	up	-0.73	0.30431758	No
PRAMEF11	ENST00000619922	4.40	0.010586296	up	-0.13	0.992833412	No
CENPA_a	ENST00000475662	4.40	0.000326357	up	-1.17	0.84823361	No
GPR37	ENST00000303921	4.39	1.19E-08	up	0.14	0.981222213	No
HSPA1A_a	ENST00000441618	4.31	0.000662654	up	-0.39	0.18443152	No
SERPINF2	ENST00000382061	4.07	6.14E-05	up	0.38	0.891316067	No
ZNF296	ENST00000303809	4.02	0.004702231	up	-0.35	0.969612411	No
RFPL4B	ENST00000441065	3.87	8.47E-08	up	-1.72	1.44E-06	Yes
PRAMEF8	ENST00000357367	3.78	0.019759829	up	-3.05	0.035391996	Yes
TRIM53AP	ENST00000532014	3.75	0.001015777	up	-0.70	0.597602437	No
CCNA1_a	ENST00000255465	3.31	3.94E-19	up	-0.37	0.463772143	No
CCNA1_b	ENST00000625767	3.27	2.05E-16	up	-0.45	0.09064676	No
PTP4A3_a	ENST00000520105	2.99	3.12E-13	up	0.43	0.166532775	No
RIPK4	ENST00000332512	2.93	6.86E-10	up	-0.03	0.995355899	No
ACKR4	ENST00000249887	2.90	0.000808967	up	-0.89	0.226235022	No
PPP2R2B	ENST00000394411	2.87	0.004828947	up	-1.23	0.845669111	No
THOC5_b	ENST00000484924	2.78	3.42E-05	up	-0.35	0.909720201	No
JUP_a	ENST00000449889	2.59	3.54E-07	up	0.21	0.957590214	No
TRIM64B	ENST00000329862	2.51	0.02102623	up	-1.45	0.077007169	No
C1QTNF3	ENST00000231338	2.41	3.24E-51	up	-0.12	0.916619331	No
HPGD	ENST00000296522	2.37	0.04900649	up	0.12	0.992774603	No
JUP_b	ENST00000591690	2.30	8.74E-07	up	0.00	0.999964077	No
PTP4A3_b	ENST00000521578	2.29	2.12E-25	up	0.58	0.002408606	No
PNMA2	ENST00000522362	2.15	1.87E-28	up	0.03	0.991303373	No
SIAH1	ENST00000356721	2.06	0.004347022	up	0.05	0.99534489	No
THOC5_c	ENST00000443089	2.05	1.24E-17	up	-0.20	0.772030789	No
TRIL	ENST00000539664	2.01	0.001074742	up	0.04	0.994199094	No
CCR4	ENST00000330953	-2.11	0.005067901	down	-0.53	0.971783714	No
MELK_a	ENST00000298048	-2.12	0.000252848	down	0.40	0.94825751	No
MTFR2_a	ENST00000420702	-2.28	0.010004786	down	1.43	0.630429768	No
GOLGA6A	ENST00000290438	-2.34	5.35E-09	down	0.50	0.791090752	No
BORA	ENST00000377815	-2.38	0.009935466	down	0.05	0.999371732	No

Table S1 (cont'd.)

Gene*	Transcript ID	Non-treated FSHD vs Healthy**			Treated FSHD vs Non-treated FSHD**		
		log2FC	adj. p-value	up/down?	log2FC	adj. p-value	significantly restored by treatment?
MTFR2_b	ENST00000451457	-2.56	0.036193589	down	-2.42	0.866364671	No
GOLGA6C	ENST00000300576	-2.63	3.60E-05	down	-0.79	0.98271602	No
MAP7D2	ENST00000379643	-3.08	2.21E-10	down	0.14	0.992774603	No
MELK_b	ENST00000626154	-3.38	0.003594245	down	-5.38	0.478787787	No
ODC1	ENST00000446285	-3.74	0.0101774	down	3.37	0.667785883	No
CDC20_a	ENST00000372462	-3.75	0.000246158	down	-0.34	0.992833412	No
SCG5_a	ENST00000475752	-3.81	2.45E-38	down	-0.71	0.776061124	No
CENPA_b	ENST00000233505	-3.83	0.012455446	down	-4.13	0.862519595	No
UBE2C_a	ENST00000356455	-3.83	5.08E-57	down	-0.24	0.944545174	No
CDC20_b	ENST00000310955	-3.98	1.25E-87	down	-0.63	0.263401187	No
SCG5_b	ENST00000498607	-3.99	1.17E-07	down	-1.28	0.967200594	No
UBE2C_b	ENST00000372568	-4.33	5.29E-07	down	1.31	0.943676285	No
CD248	ENST00000311330	-4.62	2.42E-275	down	-0.08	0.987440238	No
SYT7	ENST00000542836	-4.71	1.31E-05	down	2.44	0.868797513	No
DNER	ENST00000341772	-4.91	1.32E-88	down	-0.11	0.991213343	No
HSPA1B_c	ENST00000445736	-5.32	0.002037533	down	0.24	0.997320359	No
CENPA_c	ENST00000335756	-5.48	2.08E-06	down	2.20	0.716243485	No
HSPA1B_d	ENST00000450744	-6.14	5.68E-05	down	1.80	0.6047912	No
STIL_b	ENST00000447475	-6.84	0.025544257	down	6.90	5.84E-05	Yes
SPATA33	ENST00000579310	-7.19	7.01E-06	down	5.94	0.294771871	No

*letters after the underscore are arbitrary identifiers of different transcripts from the same gene
**this group served as reference for the comparison

Table S2. Validation of some FSHD signature genes from RNA sequencing analysis

Transcript	Status in FSHD	Significantly restored by treatment in RNA-seq?	Validated by qPCR? (status, figure)
TRIM51	up-regulated	yes	not validated
TRIM43	up-regulated	yes	yes (restored, Fig. 1C)
SLC34A2_a	up-regulated	yes	not validated
ZSCAN4	up-regulated	yes	yes (restored, Fig. 1C)
PRAMEF1	up-regulated	yes	not validated
TRIM43B	up-regulated	yes	not validated
RFPL4B	up-regulated	yes	not validated
PRAMEF8	up-regulated	yes	not validated
MBD3L2	up-regulated	no	yes (restored, Fig. 1C)
TRIM48	up-regulated	no	yes (restored, Fig. S1)
TRIM64B	up-regulated	no	yes (restored, Fig. S1)
PRAMEF4/5/9/11	up-regulated	no	yes (restored, Fig. S1)
STIL_b	down-regulated	yes	not validated

Table S3. Characteristics of the immortalized human muscle cells used in this study.

Cell ID	Disease Status	Sex	Age at biopsy	EcoRI/BlnI allele size (4q haplotype)
WS229	FSHD	Male	66 y/o	>112 kb (B) / 28 kb (A)
WS234	Healthy	Female	60 y/o	>145 kb (B) / 107 kb (B)

Table S4. Primers used for qPCR evaluation of gene expression in this study.

Gene	Forward (F) and Reverse (R) primers, 5' to 3'
DUX4	F: CCCAGGTACCAGCAGACC R: TCCAGGAGATGTAACTCTAATCCA
GAPDH	F: GCAAATTCCATGGCACCGT R: AGGGATCTCGCTCCTGGAA
BANF1	F: TGACAAGGCCTATGTTGTCC R: CACAAGTGTCTTTCAGCCATTC
SSR4	F: GCAGGCACCTATGAGGTTAG R: CTCGTTATTCCTCTGAGCCTTC
FARP1	F: GACTGCCGAGCCGCTTT R: TCTTGAGTTCGTGCAGCTTCTG
ZBTB7B	F: AAACTGCCTCGCCACAT R: CAGCTTGTCGTTCCTGGT
TRIM48	F: TATGGAGAGGAGGGACTCTTTAG R: CTACATGGTTGGTAGGTCTTGG
PRAMEF4/5/9/11	F: CCAGAGCAGAAGAAGGAGATTG R: TGGCCTTCGAGGAAAGAAAC